Journal of Environmental Management 373 (2025) 123995

Contents lists available at ScienceDirect

Journal of Environmental Management

journal homepage: www.elsevier.com/locate/jenvman

Research article

Management of wind-turbine blade waste as high-content concrete addition: Mechanical performance evaluation and life cycle assessment

Javier Manso-Morato [a], Nerea Hurtado-Alonso [b], Víctor Revilla-Cuesta [a], Vanesa Ortega-López [a,*]

[a] Department of Civil Engineering, Escuela Politécnica Superior, University of Burgos, c/ Villadiego s/n, 09001, Burgos, Spain
[b] Department of Construction, Escuela Politécnica Superior, University of Burgos, c/ Villadiego s/n, 09001, Burgos, Spain

ARTICLE INFO

Handling Editor: Prof Raf Dewil

Keywords:
Raw-crushed wind-turbine blade (RCWTB)
Fiber-reinforced concrete (FRC)
Mechanical performance
Life cycle assessment (LCA)
Prediction model

ABSTRACT

The management of end-of-life wind-turbine blades in the coming years will be necessary, as a clear solution for their recycling is yet to be found due to their complex composition. The suitability of their mechanical recycling is therefore evaluated in this paper, obtaining Raw-Crushed Wind-Turbine Blade (RCWTB) for subsequent incorporation in high amounts of up to 10% vol. in concrete, replacing the aggregates to achieve Fiber-Reinforced Concrete (FRC). Compressive strength levels of 40 MPa were at all times reached, although with steadily decreasing elastic moduli, properties that could be precisely related by regression using a hardened-density correction. Besides, tensile splitting strength increased by 0.03 MPa *per* 1% RCWTB and Poisson's coefficient was reduced, while maintaining flexural strength levels. Finally, life cycle assessment showed lower global warming potential for mixes with RCWTB, even compared to other FRC mixes, as the contents related to high-emitting raw materials of FRC were reduced. The results were promising and reveal a path towards greater sustainability of the wind-energy sector in alliance with the concrete industry.

Glossary

FRC	Fiber-Reinforced Concrete
GFRP	Glass Fiber-Reinforced Polymer
RCWTB	Raw-Crushed Wind-Turbine Blade
LCA	Life Cycle Assessment
FD	Fresh Density
OAC	Occluded Air Content
CS	Compressive Strength
TSS	Tensile Splitting Strength
FS	Flexural Strength
MoE	Modulus of Elasticity
PC	Poisson's Coefficient

1. Introduction

As time goes by, the need for industrial expansion, globalization, and specialization is growing exponentially. Industrial sectors are increasingly focused on optimal solutions where there is no overconsumption of natural resources, aiming to achieve zero waste through the recovery and reuse of resulting by-products (Ferronato and Torretta, 2019). Nevertheless, recycling waste materials within the same industry can sometimes result in higher environmental impacts than the extraction of new raw materials (Peceño et al., 2020), so a cross-sector approach to recycling must be adopted to make the circular economy a reality through all industrial sectors (Migliore et al., 2019). The concrete industry is often at the receiving end of cross-sector recycling (Behera et al., 2014), as concrete manufacturers are constantly searching for sustainable materials to incorporate in their mixes, in order to mitigate the high environmental impact of concrete (Xing et al., 2023), mainly due to cement production (ANEFHOP, 2022) and aggregate extraction (Kurda et al., 2018). Different strategies are under debate within the concrete industry to mitigate the reduction of its environmental-impact, while simultaneously addressing its cross-sector recycling:

- First, the incorporation of supplementary cementitious materials as cement replacement that are by-products of the siderurgical industry and the coal and energy sector (Juenger and Siddique, 2015), such as furnace slag (Faleschini et al., 2023; Ortega-López et al., 2022; Revilla-Cuesta et al., 2023a), silica fume (Khodabakhshian et al.,

* Corresponding author.
E-mail address: vortega@ubu.es (V. Ortega-López).

https://doi.org/10.1016/j.jenvman.2024.123995
Received 1 September 2024; Received in revised form 28 December 2024; Accepted 28 December 2024
Available online 2 January 2025

2018), and fly ash (Kurda et al., 2018; Liu et al., 2020), among many others.

- Second, reduced consumption of natural aggregate through its replacement with recycled aggregate (Martínez-Lage et al., 2020; Pradhan et al., 2019; Revilla-Cuesta et al., 2022a), as mining and extraction of natural aggregate are high-energy processes that must be mitigated to reduce their environmental impacts (Kurda et al., 2018). Those sorts of aggregates can, for example, be construction and demolition waste from the renewal and upscaling of existing infrastructure. Likewise, by-products from packaging and disposable consumer products (Gu and Ozbakkaloglu, 2016) produced in the plastics industry, also among the most highly polluting industrial processes, are also interesting sources of recovered waste (PlasticsEurope, 2019). Waste plastic by-products can also be added to the concrete mix in many different ways, one of which is as recycled plastic aggregate (Gu and Ozbakkaloglu, 2016).
- The third strategy is the addition of recovered waste as fibers to produce Fiber-Reinforced Concrete (FRC), sometimes lowering the cement content of the mix (Yuan et al., 2023). Fibers can be found in different sectors, such as the plastic industry (Mahdi et al., 2023; Yina et al., 2016) where different synthetic fiber recycling methodologies have been studied (Mahdi et al., 2023; Signorini et al., 2022; Yina et al., 2016), and the tire industry, where the steel filaments present in this product can be recycled in a non-expensive manner (Neocleous et al., 2011; Soltanzadeh et al., 2022).

The wind-energy industry has a clear need to consider ways of recycling decommissioned wind-turbine blades, as many wind-turbine blades are reaching the end of their lifespan (World Wind Energy Association, 2022). It is estimated that about 25,000 wind turbines will be decommissioned before 2050 (Beauson and Brøndsted, 2016). As much as 80% by weight of these elements can be recycled for different purposes, although a widely accepted recycling process has yet to be agreed, due to the complex composition, mainly based in Glass Fiber-Reinforced Polymer (GFRP) and high-energy demands of many recycling processes (Revilla-Cuesta et al., 2023b). Different approaches have been under study (Leon, 2023), such as blade segmentation for urban furniture (Joustra et al., 2021), and the recovery of glass fibers through physical-chemical treatments (Esmizadeh et al., 2019), although cross-sector recycling through the concrete industry is perhaps the most viable solution (Yazdanbakhsh et al., 2017).

At present, there are various alternatives for crushing wind-turbine blades prior to the incorporation of the resulting raw material in concrete. Some researchers have attempted to introduce these elements as fine or coarse aggregates (Correia et al., 2011; Hofmeister, 2012), powder (Baturkin et al., 2021), and fibers (Revilla-Cuesta et al., 2023b, 2024b), all of which are sustainable ways of avoiding the high environmental impacts of landfilling wind-turbine blades (World Wind Energy Association, 2022). More precisely, the incorporation of fibers within concrete is a viable alternative to the recycling of the GFRP composites within the blades. It is also an economic and an environmentally efficient way of improving the mechanical properties of this construction material (Revilla-Cuesta et al., 2024b). Furthermore, the fibers can even be obtained by non-selective cutting and milling of the whole blade, with no component separation, thereby producing a material known as Raw-Crushed Wind-Turbine Blade (RCWTB) (Revilla-Cuesta et al., 2023b). Concrete mixes containing high-percentages of RCWTB are investigated in this research. A novel approach towards its incorporation was adopted: RCWTB was added without modifying the cement amount, in order to achieve a balance between the mechanical and environmental performance of the concrete produced with this by-product.

Life Cycle Assessment (LCA) plays a pivotal role in cross-sector recycling for concrete production (Vieira et al., 2016). A properly performed LCA is key to any clear environmental assessment of the treatments to which the waste materials have to be subjected before their incorporation in a concrete mix (EN-Euronorm, 2020). The need for preparation and manipulation of some residues can even result in higher environmental impacts than conventional concrete (Mahdi et al., 2023). Moreover, some by-products may weaken the mechanical properties of concrete due to their low quality (Mahdi et al., 2023). Thus, LCA is an important decision-making tool to determine which scenarios in cross-sector recycling are beneficial (Hay and Ostertag, 2018), an aspect that also has to be analyzed in the case of the wind-energy sector (Nagle et al., 2020).

In this novel research, the effects of incorporating up to 10% RCWTB in concrete mixes without modifying the cement amount are studied. The results for fresh-state features (Section 3.1), and 28-day mechanical properties (Section 3.2) are discussed in this paper, in order to fully characterize the different mixes. Then, a statistical analysis of the relations between those properties (Section 4) and an LCA of all the mixes (Section 5) are conducted. The main goal of this research is to understand the complete behavior of concrete incorporating high contents of RCWTB, both in mechanical and environmental terms. In this way, the aim is to find a solution to the wind-energy industry through cross-sector recycling in the concrete industry.

2. Materials and methods

2.1. Raw materials

The concrete mixtures used CEM II/A-L 42.5 R, as *per* EN 197-1 (EN-Euronorm, 2020), which consisted of ordinary Portland cement with a slight reduction of the clinker content (6–20% of limestone). The characteristics of all the aggregates can be seen in Table 1. A gradation of each aggregate fraction was carried out in line with EN 933-1 (EN-Euronorm, 2020), graphed in Fig. 1. Tap water was used, and two different admixtures (a high-range water reducer and a superplasticizer) were incorporated, in order to maintain low water/cement ratios, and to ensure that all mixtures had proper fresh and mechanical properties (Barbudo et al., 2013).

The RCWTB recycling process and its composition have been thoroughly discussed in previous works of the authors (Revilla-Cuesta et al., 2023b). This recycling process involved the cutting of decommissioned wind-turbine blades, composed of GFRP composites mixed with polymeric resins and balsa wood (Joustra et al., 2021), into regular-shaped pieces, and their subsequent non-selective crushing. RCWTB contained GFRP-composite fibers with an average length of 13.1 mm (66.8% wt.); balsa wood (6.3% wt.) and polymeric semispherical particles (8.3% wt.); microfibers (13.8% wt.); and small non-separable particles (4.8% wt.). The apparent density of RCWTB was 246.64 kg/m^3.

The cost to produce RCWTB is actually 41% cheaper than the average energy consumption for quarry extraction of natural crushed aggregate (Petit et al., 2018; Revilla-Cuesta et al., 2023b). The RCWTB production process involved cutting and crushing of the whole blade into smaller, more manageable particles, whose energy cost was estimated at 1.23 kWh/metric ton of RCWTB (Revilla-Cuesta et al., 2023b). Accounting for a cost of 0.20 €/kWh in Spain, a metric ton of RCWTB for use as raw material in concrete production could cost around 0.25€.

Table 1
Physical characteristics of natural aggregates.

Aggregates	Nature	SDD Density (kg/m^3)	24-h water absorption (%)
Gravel 12/22	Siliceous	2.60	0.55
Gravel 4/12	Siliceous	2.63	0.32
Sand 0/4	Siliceous	2.62	0.13
Sand 0/2	Limestone	2.66	0.10

SSD: Saturated Surface Dry.

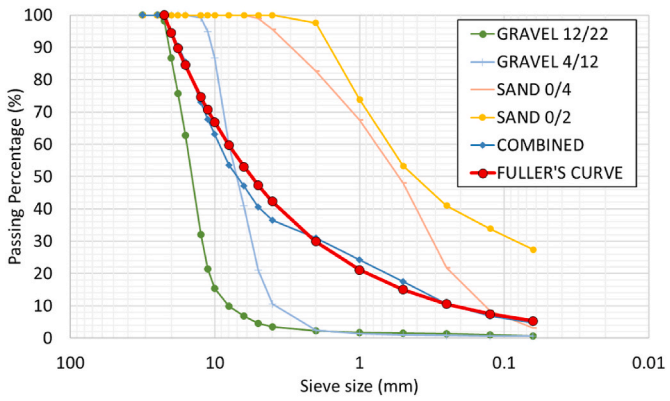

Fig. 1. Individual and combined gradation of the aggregates, alongside the Fuller's curve.

2.2. Mix design and production

In all, 11 different mixes were manufactured for this research. A reference mix without RCWTB, prepared and labelled W0 (0% RCWTB), was designed in accordance with European and Spanish regulations (European Committee for Standardization, 2010; Ministry of Infrastructures of the Spanish Government, 2021), to achieve an S3 slump classification (slump of 100–150 mm) according to EN 12350 (EN-Euronorm, 2020). The proportions of the different aggregate fractions were defined in an adjustment to the Fuller's Curve (Fig. 1). RCWTB was added in steps of 1% vol. for the remaining 10 mixes, maintaining the cement content and the proportion of each natural aggregate fraction constant. RCWTB consists of a variety of particulate proportions that can complement different aggregate sizes (Revilla-Cuesta et al., 2023b). The mixes were labelled W1 to W10. The decision to incorporate RCWTB without varying the cement amount was taken to balance the mechanical properties of the concrete and the LCA (Acosta-Calderon et al., 2022; Frazão et al., 2022).

Fiber additions usually hinder proper workability and adequate slump (Habert et al., 2013). Nevertheless, both properties were ensured in all the mixes through empirical adjustments to the water and the admixture contents, as the RCWTB content was raised. Those changes are reported both in Fig. 2 and in Table 2, and are adjusted to a cubic meter in Table 3. An increased amount of water was adequate for low RCWTB contents. However, admixture proportions were increased from mix W5, to avoid excessive water additions when using high RCWTB contents, which might otherwise negatively affect the strength performance of the concrete samples (Mousavi et al., 2019). These admixtures reduced the amount of water needed to ensure suitable fresh state characteristics of FRC (Abdolpour et al., 2023; Frazão et al., 2022).

A three-step process was specifically designed, to ensure the homogeneity of the mixing process (Acosta-Calderon et al., 2022), in order to achieve proper hydration of all raw-materials and homogeneity of the mix (Revilla-Cuesta et al., 2023b) (Fig. 3). First, the water quantity was segmented into three distinct portions: the first portion was 0.50 L, while the other two portions allocated 30% and 70% of the remaining water of each specific mixture, respectively. The mixer was then pre-moistened, and several mixing steps were conducted. In the initial step, all the aggregates combined with the 30% water portion were introduced and mixed together for 5 min. Then, the cement and the RCWTB were introduced into the mixer, along with water in a proportion of 70%, and mixing for another 3 min. Afterwards, having been dissolved in the 0.50 L of water, the admixtures were incorporated into the mixture and mixed for a further 5 min. To verify the desired workability, a slump test was conducted following EN 12350-2 (EN-Euronorm, 2020) upon completion of all the mixing stages.

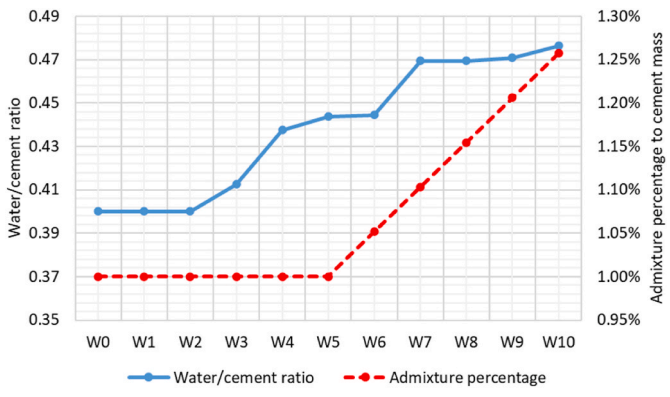

Fig. 2. Water/cement ratio and admixture percentage of the cement mass.

2.3. Experimental plan

Firstly, the manufactured concrete mixes were evaluated in terms of slump (EN 12350-2 (EN-Euronorm, 2020)), Fresh Density (FD) (EN 12350-6 (EN-Euronorm, 2020)), and Occluded Air Content (OAC) (EN 12350-7 (EN-Euronorm, 2020)). Meanwhile, specimen casting for evaluating the hardened-state performance took place in accordance with standard EN 12390 (EN-Euronorm, 2020). Three specimens were manufactured for each test, and were only used after 28 days of curing: (1) cubic specimens with a side length of 100 mm for Hardened Density (HD); (2) cylindrical specimens with a height of 200 mm and a height/diameter ratio of 2 for compressive strength (CS), tensile splitting strength (TSS), modulus of elasticity (MoE), and Poisson's coefficient (PC); and (3) prismatic specimens of 275 mm in length and a cross-section of 75 mm by 75 mm for flexural strength (FS). All the specimens were demolded after 24 h and stored in a humid chamber in accordance with EN 12390-2 (EN-Euronorm, 2020).

Moreover, the validity of current regulations to estimate the mechanical properties of RCWTB concrete was assessed. To that end, the experimental values of those properties were compared with the theoretical values of standards used in Spain, Europe, and the USA, while trying to predict the mechanical behavior of the concrete through a correlation analysis and model adjustment. Afterwards, an LCA of the 11 mixes was completed, in order to better understand the environmental performance of all mixes and their potential impacts related to the influence of their raw materials.

2.3.1. Prediction formulas from regulations

The Spanish (Ministry of Infrastructures of the Spanish Government, 2021), the European (European Committee for Standardization, 2010), and the American regulations (American Concrete Institute, 2019) contain different formulations to predict various mechanical characteristics of the concrete. Those formulations were designed for conventional concrete, so their validity and accuracy should be proven in order to be applied for the prediction of MoE (Table 4), TSS (Table 5) and FS (Table 6) in FRC incorporating RCWTB.

The Spanish regulations, known as the Spanish Structural Code (SC) (Ministry of Infrastructures of the Spanish Government, 2021), have been applied in Spain to all construction materials since 2021, and are, in terms of their specifications on concrete, based upon Eurocode 2 (EC2) Part 1-1 (European Committee for Standardization, 2010). Their expressions consider the compressive strength at the reference age (usually 28 days), the type and strength of the cement used for concrete manufacturing, and the age at which the characteristic has to be predicted. In contrast, the expressions of the American Concrete Institute standards (ACI 318-19 (American Concrete Institute, 2019)) are based on experimental factors applied to compressive strength testing.

Table 2
Comparative composition of the manufactured mixes (kg).

Mix	W0	W1	W2	W3	W4	W5	W6	W7	W8	W9	W10
Cement	320	320	320	320	320	320	320	320	320	320	320
Water	128	128	128	132	140	142	142	150	150	151	152
Admixture 1	1.07	1.07	1.07	1.07	1.07	1.07	1.12	1.17	1.23	1.28	1.33
Admixture 2	2.13	2.13	2.13	2.13	2.13	2.13	2.25	2.36	2.47	2.58	2.69
Gravel 12/22	780	772	764	757	749	741	733	725	718	710	702
Gravel 4/12	555	549	544	538	533	527	522	516	511	505	500
Sand 0/4	385	381	377	373	370	366	362	358	354	350	346
Sand 0/2	280	277	274	272	269	266	263	260	258	255	252
RCWTB	0	12	25	37	50	62	75	87	99	112	124

Table 3
Composition of the manufactured mixes *per* cubic meter (kg/m^3).

Mix	W0	W1	W2	W3	W4	W5	W6	W7	W8	W9	W10
Cement	320	320	320	319	316	315	315	313	313	313	312
Water	128	128	128	131	138	140	140	147	147	147	149
Admixture 1	1.07	1.07	1.07	1.06	1.05	1.05	1.10	1.15	1.20	1.25	1.30
Admixture 2	2.13	2.13	2.13	2.12	2.11	2.10	2.21	2.30	2.41	2.52	2.62
Gravel 12/22	780	772	764	753	740	730	723	709	701	693	684
Gravel 4/12	555	549	544	536	526	520	514	505	499	493	487
Sand 0/4	385	381	377	372	365	361	357	350	346	342	338
Sand 0/2	276	273	271	267	262	259	256	251	248	246	242
RCWTB	0	12	25	37	49	61	74	85	97	109	121

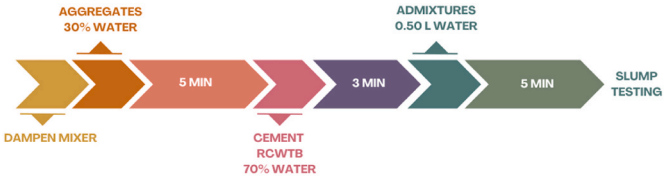

Fig. 3. Mixing process timeline.

Table 4
Formulations for estimating the Modulus of Elasticity (MoE) in each of the regulations.

Regulations	Formulation
EC2	$E_{cm}(t) = \beta_{cc}^{1/3}(t) * E_{cm}$ $\beta_{cc}(t) = \exp\left[s_c\left(1 - \sqrt{\frac{t_{ref}}{t}}\right)\sqrt{\frac{28}{t_{ref}}}\right]; t \leq t_{ref}$ $E_{cm} = k_E * f_{cm}^{1/3}$
SC	$E_{cm}(t) = \left(f_{cm}(t)/f_{cm}\right)^{0.3} * E_{cm}$ $f_{cm}(t) = \beta_{cc}(t) * f_{cm}$ $\beta_{cc}(t) = \exp\left[s\left(1 - \sqrt{\frac{28}{t_{ref}}}\right)\right]$
ACI 318-19	$E_{cm} = 4,700 * \sqrt{f_{cm}}$

$E_{cm}(t)$: Secant modulus of elasticity of concrete at age t; $\beta_{cc}(t)$: Coefficient for determining the compressive concrete strength, which depends on the age of the concrete t; E_{cm}: Secant modulus of elasticity of concrete; s_c: Coefficient for different early strength development of concrete and concrete strength; k_E: Adjustment factor for the modulus of elasticity of concrete considering the type of aggregates; f_{cm}: Mean concrete cylinder compressive strength at age t_{ref}; s: Coefficient dependent on cement type (American Concrete Institute, 2019; European Committee for Standardization, 2010; Ministry of Infrastructures of the Spanish Government, 2021).

Table 5
Formulations for estimating Tensile Splitting Strength (TSS) in each of the regulations.

Regulations	Formulation
EC2	$f_{ctm}(t) = \beta_{cc}^{0.6}(t) * f_{ctm}$
SC	$f_{ctm}(t) = (\beta_{cc}(t))^{\alpha} * f_{ctm}$
ACI 318-19	$f_{ctm} = 0.56 * f_{cm}^{0.5}$

f_{ctm}: Mean axial tensile strength of concrete at age t_{ref}; $f_{ctm}(t)$: Tensile strength of concrete at age t; f_{ck}: Characteristic concrete cylinder compressive strength at age t_{ref}; α: Factor depending on concrete age (American Concrete Institute, 2019; European Committee for Standardization, 2010; Ministry of Infrastructures of the Spanish Government, 2021).

Table 6
Formulations for estimating Flexural Strength (FS) in each of the regulations.

Regulations	Formulation
EC2	$f_{ctm,fl} = max\left\{\left(1.6 - \frac{h}{1000}\right)f_{ctm}; f_{ctm}\right\}$
SC	$f_{ctm,fl} = max\left\{\left(1.6 - \frac{h}{1000}\right)f_{ctm}; f_{ctm}\right\}$
ACI 318-19	$f_{ctm,fl} = 0.94 * f_{cm}^{0.5}$

$f_{ctm,fl}$: Mean flexural tensile strength of concrete; h: Overall depth of a cross-section or of a part of a cross-section (American Concrete Institute, 2019; European Committee for Standardization, 2010; Ministry of Infrastructures of the Spanish Government, 2021).

3. Experimental results and discussion

3.1. Fresh-state properties

3.1.1. Slump

Slump tests were performed to gain a better understanding of the effects of fiber additions on the workability of concrete (Ali et al., 2023), as they usually hinder it considerably (Sahmaran et al., 2005). All the slumps and their respective mixes can be seen in Table 7 that were all

Table 7
Slumps of the manufactured concrete mixtures.

Mix	W0	W1	W2	W3	W4	W5	W6	W7	W8	W9	W10
Slump (cm)	14.7	14.0	13.5	10.0	13.0	13.0	10.1	13.1	12.0	10.0	12.2

classified as S3 slump category (10–15 cm).

As depicted in Fig. 2, water and admixture contents were empirically adapted to achieve the desired workability, according to which four main groups could be differentiated:

- Mixes W0, W1, and W2: these mixes had equal amounts of water and admixtures, and the slump therefore decreased proportionally with the amounts of RCWTB.
- Mixes W3, W4, and W5: additional amounts of water were added to maintain the S3 slump class (slump of 10.0 cm in the W3 mix), as is usual when sustainable fibers are added (Acosta-Calderon et al., 2022).
- Mixes W6, and W7: the water amount was increased, but an increasing quantity of admixtures was imperative to maintain the workability without excessive water/cement ratios (Ali et al., 2023).
- Mixes W8, W9, and W10: additions of slightly larger amounts of admixtures were decisive in achieving an adequate slump, while the water content remained almost constant, so that the mechanical performance was not hindered (Revilla-Cuesta et al., 2023b, 2024b).

3.1.2. Fresh density

FD results are shown in Fig. 4a. The FD decreased linearly with the addition of RCWTB, due to the lower density of this recovered waste, mainly due to the particles of balsa wood and polymers, and the increasing amounts of water and admixtures (Revilla-Cuesta et al., 2023b, 2024b). Mix W10 therefore showed a decrease in FD of 7.44% compared to the reference mix W0. Nevertheless, there was a 0.41% increase in FD in mixes W1 and W2 compared to mix W0, the FD remaining almost constant between both. This behavior might be because of a slight improvement in the compactness of the cementitious matrix, due to the low proportion of fine particles within RCWTB (Nedeljković et al., 2021; Revilla-Cuesta et al., 2023b; Kirthika et al., 2020).

3.1.3. Occluded air content

The OAC results are presented in Fig. 4b. The reference mix had the lowest value, 2.2% OAC, and mix W10 had the highest value, at 4.2%. The addition of RCWTB negatively affected OAC, which slightly increased by 3.91% *per* 1% of added waste, in an overall trend when analyzing all the data simultaneously. Nevertheless, that property was highly variable when adding RCWTB (Revilla-Cuesta et al., 2024b) and there were various local trends between different amounts of RCWTB added to the mixes that were not accurately reflected by the general trend. However, these OAC values were always higher than in the reference mix. Fiber additions will commonly favor air entrainment within the cementitious matrix of concrete, as the same tendencies were found in other research with conventional fibers (Alsaif and Alharbi, 2022), sustainable fibers (Mahdi et al., 2023) and even RCWTB (Revilla-Cuesta et al., 2024b), thus creating a more porous matrix (Revilla-Cuesta et al., 2024a).

3.2. Hardened-state properties

3.2.1. Hardened density

HD results at a curing age of 28 days (Table 8) showed a decreasing trend with the RCWTB additions, from regular values in mix W0 (European Committee for Standardization, 2010; Ministry of Infrastructures of the Spanish Government, 2021) to a 5.35% reduction in mix W10, for the reasons explained in Section 3.1.2. The reduction in density was less than in previous research (Revilla-Cuesta et al., 2024b), in which mixes W3 and W6 underwent decreases in HD of 2.10% and 5.40%, respectively, compared to 1.65% and 2.88% in this study. A phenomenon that might, as mentioned above, be explained by the better compaction of RCWTB concrete (Revilla-Cuesta et al., 2023b).

Another aspect to be highlighted is that the FD and the HD were almost equal with RCWTB contents of up to 5%, while the HD was higher than the FD for higher waste contents. There was a 1.27% reduction in density from the hardened to the fresh state for mix W6, and 2.61% for mix W10. It could be explained by the high-water absorption levels of balsa wood (Sadler et al., 2009), present in larger amounts in concrete with RCWTB additions of 6% or more. The balsa wood particles could act as water accumulation points that slow water evaporation, thereby conditioning the overall density of the concrete (Revilla-Cuesta et al., 2024a).

3.2.2. Compressive strength

Graphs of compressive strength at 28-days are shown in Fig. 5a. In general, those results showed a weakening of CS with higher amounts of RCWTB, a similar trend as when adding other recycled materials (Soltanzadeh et al., 2022; Zhong and Zhang, 2020). Overall, decreasing values of 0.82 MPa in CS *per* 1% RCWTB were obtained, although mix W2 slightly deviated from that trend. Furthermore, the CS differences of the mixes with RCWTB contents of between 4% and 10% only deviated by about 4% from the mean value, showing an almost horizontal trend, observed in previous research (Revilla-Cuesta et al., 2024b). This performance demonstrated that incorporating high contents of RCWTB in concrete was possible without hindering its compressive behavior. All the mixes were suitable for structural applications (European Committee

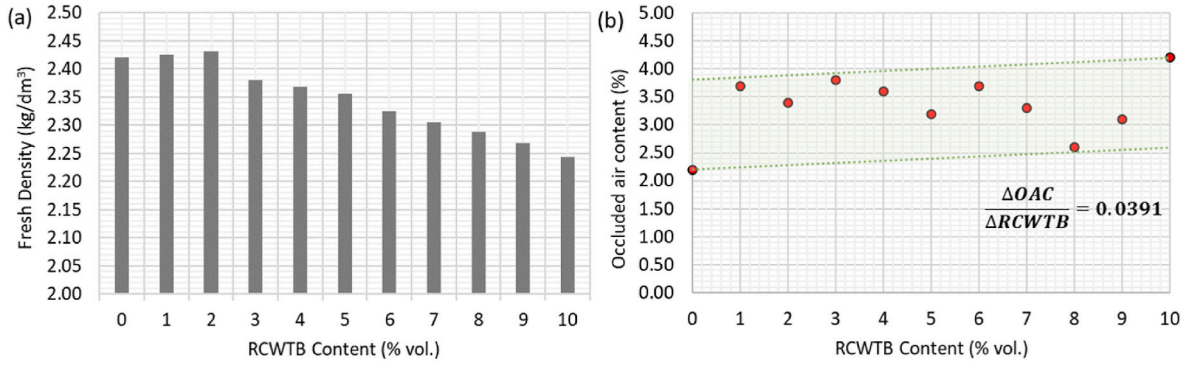

Fig. 4. Fresh-state properties: (a) FD testing; (b) OAC testing.

Table 8
HD testing.

Mix	W0	W1	W2	W3	W4	W5	W6	W7	W8	W9	W10
Hardened density (kg/dm^3)	2.43	2.43	2.42	2.39	2.37	2.36	2.36	2.33	2.31	2.30	2.30

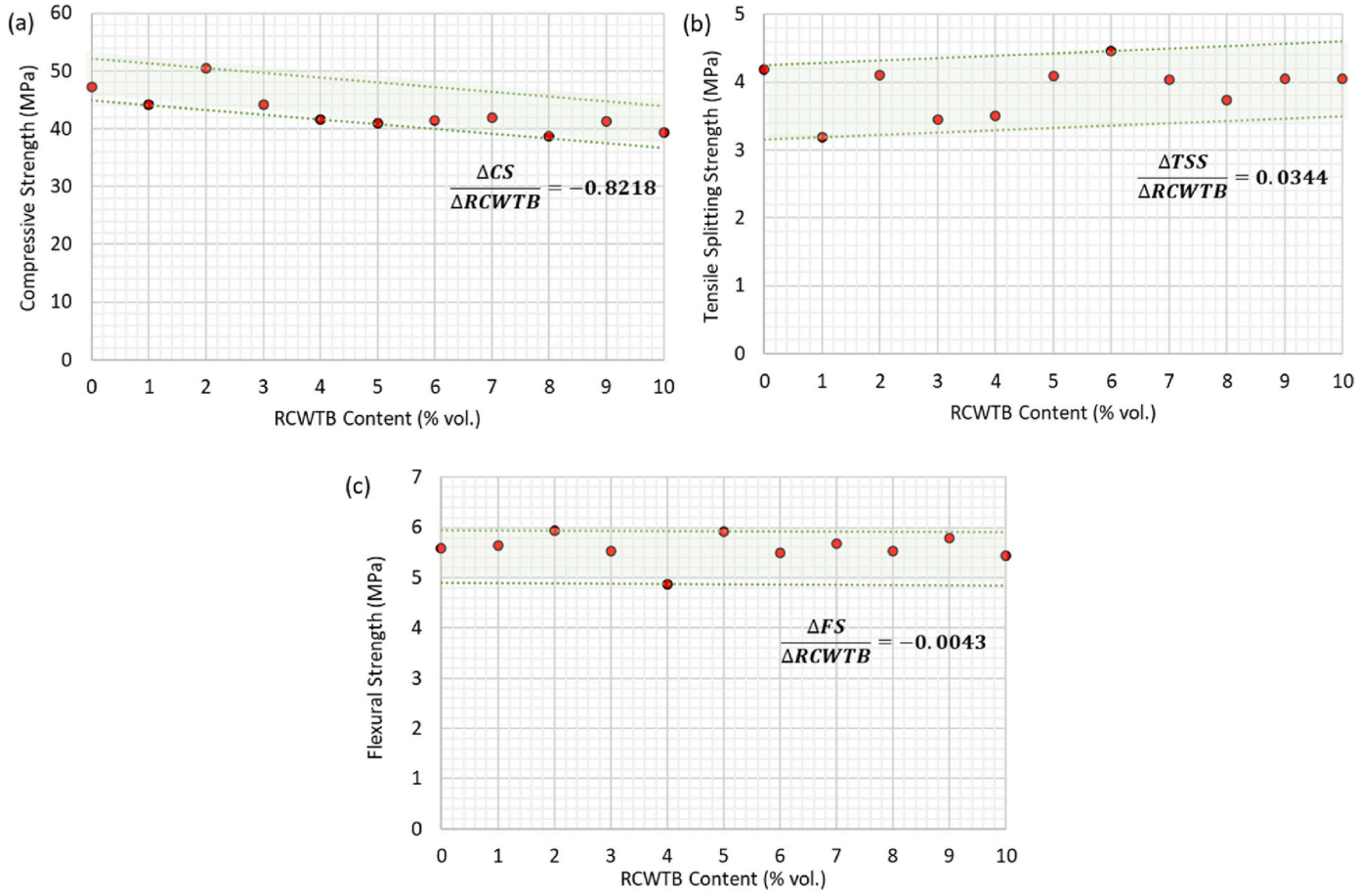

Fig. 5. Mechanical strength properties at 28 days: (a) CS testing; (b) TSS testing; (c) FS testing.

for Standardization, 2010; Ministry of Infrastructures of the Spanish Government, 2021).

This general weakening of compressive behavior could be explained by the three following factors:

- The addition of sustainable fibers is known to result in weaker compressive strength behavior (Mahdi et al., 2023), as those fibers are less efficient at resisting compressive stress (Muthukumarana et al., 2023).
- Higher amounts of water and admixture were incorporated in the mixes with high percentages of RCWTB, which negatively affected compressive strength (Miller et al., 2016).
- Balsa wood and polymeric spheres did not show proper adhesion within the cementitious matrix (Revilla-Cuesta et al., 2024b). Moreover, those particles underwent swelling and high-water retention when mixed with water, which after curing led to less dense and more porous matrices of lower compressive strength (Sadler et al., 2009).

The optimal percentage for CS was 2% RCWTB, as that amount produced compressive strengths of 50.46 MPa. It seemed to be the threshold for optimal fine particles that could assure compactness of the cementitious matrix without the incorporation of such high amounts of balsa wood and polymer particles that might negatively impact mechanical behavior (Nedeljković et al., 2021; Kirthika et al., 2020).

3.2.3. *Tensile splitting strength*

The results of TSS testing can be seen in Fig. 5b. The addition of GFRP-composite fibers from RCWTB into the concrete contributed to a three-dimensional reinforcement that avoided brittle failure of the specimens (Ali et al., 2023), as usually happens for plain concrete due to its low tensile strength (Ali et al., 2023). Those fibers therefore led to a slightly increasing trend in TSS of 0.03 MPa *per* 1% vol. RCWTB. However, that trend was not very precise, as the concrete showed various local trends within the results, with values above and below the value of the reference mix W0. Furthermore, the RCWTB fibers increased the ductility of the mixes. W0 suffered from brittle failure, as depicted in Fig. 6a, while the strongest mix (W6, with a TSS of 4.46 MPa) only suffered from hair-like cracks upon failure (Fig. 6b), a behavior that was replicated in all the mixes incorporating RCWTB.

Despite the general trend, the TSS results were disperse, showing many local trends (Fig. 5b). Such varied behavior may be explained by the scattered length of the GFRP-composite fibers and microfibers in the RCWTB (Revilla-Cuesta et al., 2023b). Furthermore, the balsa wood and polymer spheres impacted negatively due to their low density and poor adhesion within the cementitious matrix (Revilla-Cuesta et al., 2024b),

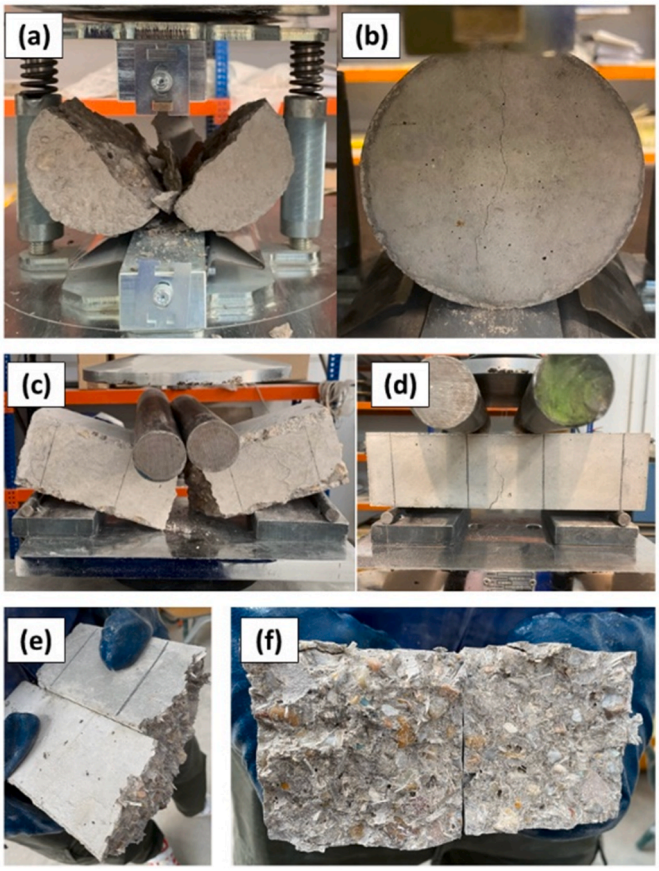

Fig. 6. Tested specimens: (a) TSS specimen failure for the reference mix W0; (b) TSS specimen failure for mix W6; (c) FS specimen failure for mix W0; (d) FS specimen failure for mix W6; (e) specimen failure of mix W10 after FS testing and opened afterwards; (f) cross-section of a specimen of mix W10 under FS testing.

which is a key factor towards high TSS (Islam et al., 2022). Finally, the varying water/cement ratios and admixture quantities for different percentages of RCWTB might also favor that performance.

3.2.4. Flexural strength

28-day FS test results (Fig. 5c) showed an almost horizontal trend, thus the GFRP-composite fibers contained in the RCWTB helped to compensate the negative effects of the increased water/cement ratios and the additional balsa wood and polymer particles (Ali et al., 2023). As FS testing combines both compression and tensile behaviors, mix performance could be explained by the detrimental effects of RCWTB for CS and the improved TSS, as mentioned above. The highest FS value, 5.94 MPa, was achieved in mix W2, which was a 6.26% higher than in the reference mix W0. That mix showed the highest value of CS and a TSS that was only 8.07% lower than the highest value, showing that both strengths were decisive in flexural behavior.

Besides, mix W6 showed the same failure mode as for TSS testing (Fig. 6c and d). The RCWTB fibers situated parallel to the longitudinal axis of the specimens (Fig. 6e and f) resulted in proper bridging of the cementitious matrix (di Prisco et al., 2009).

3.2.5. Modulus of elasticity

The stiffness evaluation of the concrete mixes at 28 days was first studied by the determination of the MoE, whose results are shown in Fig. 7a. Axial loading strain levels were measured with three longitudinal strain gauges (EN-Euronorm, 2020). The results showed a clear decreasing trend with the RCWTB amount, in which the highest value, 45.25 GPa, was recorded in the reference mix W0 and the lowest value, 33.79 GPa, in mix W10. That variation represented a decrease in the MoE of 25.33%, which was coincident with previous research (Revilla-Cuesta et al., 2024b). All the results were well above 30 GPa, the minimum strength according to structural standards (European Committee for Standardization, 2010).

A closer look at the trends revealed a slight decrease in the MoE of around 5% with up to RCWTB contents of 4%. Then, there was a sudden decrease of 16.22% for mix W5, and the decrease remained approximately constant around 20% for RCWTB amounts between 6% and 10%. The high deformability of balsa wood and polymers meant that the mixes incorporating higher amounts of RCWTB (Sadler et al., 2009) registered higher strain levels, which could only be partially compensated by GFRP-composite fibers at low percentage additions of RCWTB (Revilla-Cuesta et al., 2024b). The lower quality of the cementitious matrix, due to higher water/cement ratios when increasing the RCWTB amount, also favored such behavior. Finally, the RCWTB fibers do not work efficiently under compressive stress. The fibers therefore had no influence on the elastic behavior of the specimens when high proportions of balsa wood and polymers were incorporated (Muthukumarana et al., 2023).

3.2.6. Poisson's coefficient

The PC was measured through the MoE at 28 days (Fig. 7b). To do so, three additional transverse strain gauges were located at mid-height on the specimens (EN-Euronorm, 2020). All the PC values were below 0.20, which is the standard value in regulations for this property (EN-Euronorm, 2020; Ministry of Infrastructures of the Spanish Government, 2021), yet still in most cases relatively close to that value. The concrete mixes showed very slight negative variations with increasing RCWTB amounts.

As with previous research (Revilla-Cuesta et al., 2024b), lower PC values were obtained with RCWTB contents of up to 7%, as

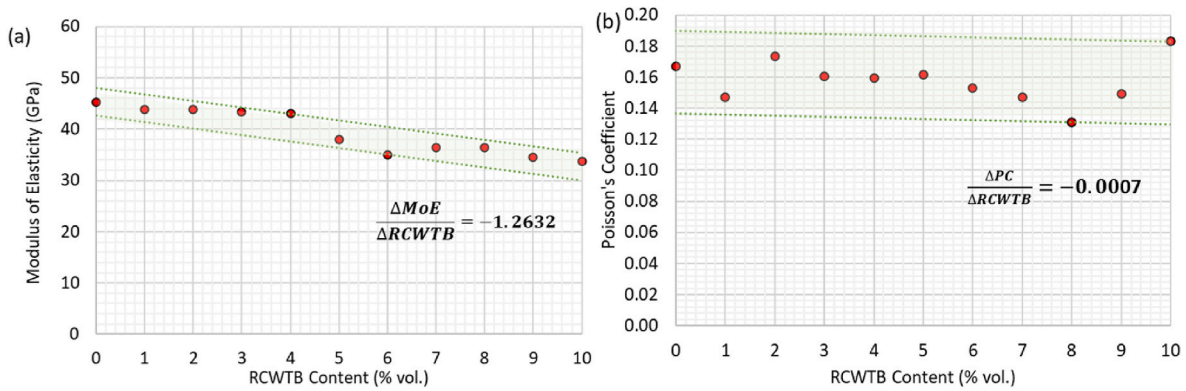

Fig. 7. 28-day stiffness evaluation: (a) MoE testing; (b) PC testing.

GFRP-composite fibers helped limit specimen bulging, due to the tensile stresses that they experienced (Shilov et al., 2021). However, higher bulging was evident in the specimens with 8% or more RCWTB, due the high deformability of balsa wood and polymer particles, which the bridging effect of the fibers was unable to compensate (Sadler et al., 2009). Thus, the highest PC value, which was 9.58% higher than that of the reference mix W0, was recorded for mix W10.

4. Prediction of mechanical performance

4.1. Correlations

Pearson's correlation coefficients were calculated for an initial evaluation of the relationships between the mechanical properties and the RCWTB content (Schober et al., 2018). This coefficient always ranges between +1 and −1: when positive, it shows a direct proportionality between the two factors under study, and when negative, it shows an indirect proportionality (Schober et al., 2018). The proportionality is more intense when its absolute value is closer to 1. The coefficients of correlation between the mentioned properties are expressed below in a heatmap (Fig. 8).

4.1.1. RCWTB content

The correlations between the RCWTB content and the mechanical properties are expressed in Fig. 8a. Three different trends can be appreciated, which corroborate the discussion in previous sections. First, a clear negative effect of RCWTB on CS and MoE can be seen, which is also reflected in the literature for other recycled materials that followed similar trends (Khelifa et al., 2021; Soltanzadeh et al., 2022). Second, there was a very slight decrease of FS and PC when adding RCWTB, as even though the fibers present in the RCWTB might benefit those properties (di Prisco et al., 2009; Shilov et al., 2021), the presence of balsa wood and polymer particles weakened FS and lowered the PC (Sadler et al., 2009). Finally, there was a moderate positive effect of RCWTB on TSS, which was the property that the GFRP-composite fibers present in the RCWTB affected most notably (Merli et al., 2020; Revilla-Cuesta et al., 2024b).

4.1.2. Mechanical properties

All the correlation coefficients between the mechanical properties can be seen in Fig. 8b. The majority of values were representative of a slight direct proportionality, with a few of them showing no relationship (CS – TSS, FS – MoE, FS – PC). The highest positive correlation was found between CS and MoE, as they jointly conditioned the compressive behavior of the concrete containing the recycled materials (Silva et al., 2016). The other notable correlation coefficient was obtained between MoE and TSS, as the higher the RCWTB amount, the larger the improvement in concrete tensile performance (Shi et al., 2020) and the higher the longitudinal deformability (Revilla-Cuesta et al., 2024b). Thus, somewhat of a negative linear relationship between both properties was revealed.

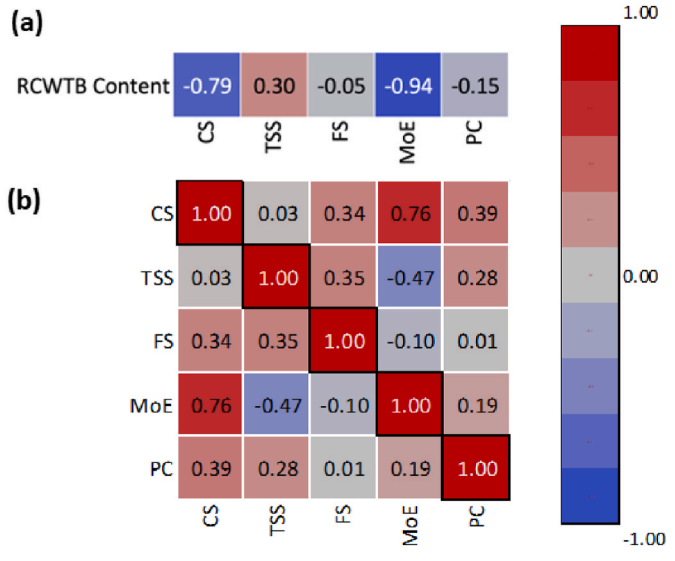

Fig. 8. Correlation coefficients: (a) RCWTB content related to mechanical properties; (b) mechanical properties compared between each other.

4.2. Validity of current regulations

The validity of current regulations (formulations in Table 4) for estimating the mechanical properties of concrete (MoE, TSS, and FS) according to CS can be evaluated with the information shown in Fig. 9. Those results yielded the following conclusions:

- The formulations of both the Eurocode 2 (European Committee for Standardization, 2010) and the Spanish Structural Code (Ministry of Infrastructures of the Spanish Government, 2021) estimated MoE in a proper manner (Fig. 9a), as the higher deviation between the experimental and the estimated values was 10.52%. However, MoE was always predicted below the experimental values for ACI 318-19 (American Concrete Institute, 2019), where the highest error was 40.20%, although it guaranteed a safe estimation in all cases. Overall, the prediction of MoE through CS was not highly influenced by the incorporation of RCWTB.
- All three regulations yielded similar estimations of TSS as a function of CS (Fig. 9b). In fact, Eurocode 2 (European Committee for Standardization, 2010) and ACI 318-19 (American Concrete Institute, 2019) almost provided the same estimated values, the higher deviation of the experimental results being 19.28% in absolute value. Meanwhile, the Structural Code (Ministry of Infrastructures of the Spanish Government, 2021) severely underestimated the experimental results, the maximum error being 30.49%.
- Lastly, all three formulations yielded acceptable estimations of FS according to CS (Fig. 9c). Eurocode 2 (European Committee for Standardization, 2010) and Structural Code (Ministry of Infrastructures of the Spanish Government, 2021) used the same formulas, reaching errors as high as +12.73%. The ACI 318-19 formula (American Concrete Institute, 2019) yielded results that overestimated all values, with errors of up to +24.44%.

4.3. Model development

As described in Section 4.1, the highest correlation between mechanical properties was reached between MoE and CS (+0.76). In addition, the ACI 318-19 formulation (American Concrete Institute, 2019) was not very accurate for estimating MoE as a function of CS. Thus, a model to predict MoE as a function of CS in RCWTB concrete was developed to improve the estimation accuracy.

4.3.1. Simple regression

First, a simple regression model was adjusted (CS in MPa, and MoE in GPa), which is shown in Equation (1). As *per* Table 9, the low R^2 value of this model at a 95% confidence level, suggested that it could not properly explain the experimental variability of MoE. The Mean Absolute Error (MAE) was normal, yet the residuals were not autocorrelated according to the Durbin-Watson Statistic.

$$MoE = 85.10 - \frac{1947.08}{CS} \quad (1)$$

4.3.2. Simple regression with correction

Then, a correction to the previous model was introduced to guarantee accurate theoretical values (Yu et al., 2021). In this model,

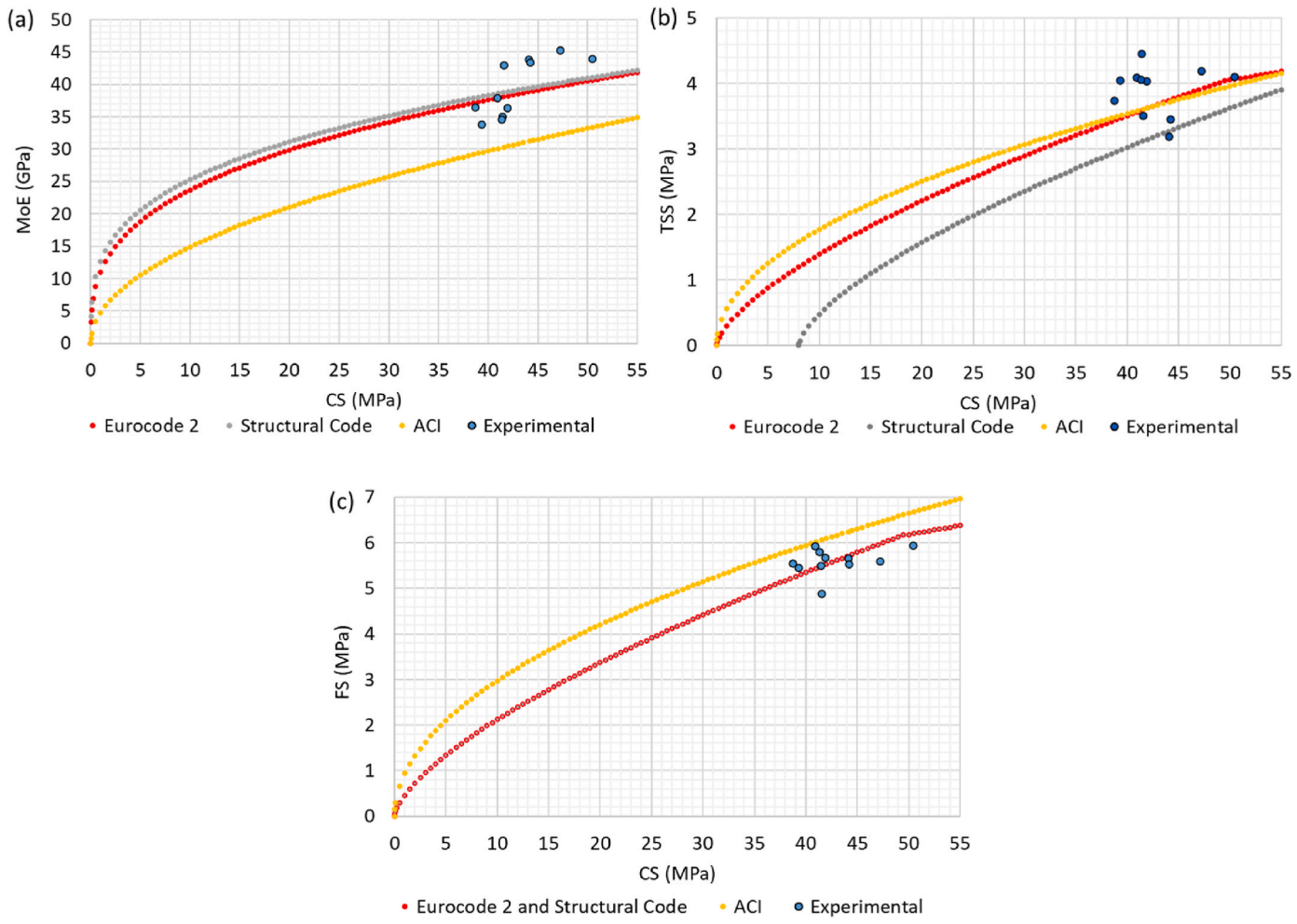

Fig. 9. Comparison of experimental values and values predicted through current regulations (American Concrete Institute, 2019; European Committee for Standardization, 2010; Ministry of Infrastructures of the Spanish Government, 2021): (a) MoE; (b) TSS; (c) FS.

Table 9
Significance statistical parameters for both regression models.

Model	Simple regression	Simple regression with correction
R^2 (%)	60.77	83.60
Mean Absolute Error	2.42	2.22
Durbin-Watson Statistic	1.77	1.60
Limit of Durbin Watson Statistic	1.32	1.32

A Durbin-Watson statistic over the limit indicates no autocorrelation of the residuals.

expressed in Equation (2), the HD results, in kg/dm^3, were used as a correction factor (Revilla-Cuesta et al., 2022b), due to the positive correlation between MoE and HD.

$$MoE = \left(0.53 + \frac{0.22}{CS}\right) * HD^5 \quad (2)$$

The deviations between the experimental values and those estimated through Equation (2) can be studied in Fig. 10. The average deviation between the experimental and the theoretical values was only 3.11%, which is represented by the green region in Fig. 10. 64% of the mixes showed a deviation lower that the average one. A ±10% deviation was represented by the red region, all the estimated values being inside this range. It represented a lower maximum deviation than the models depicted in Eurocode 2 (European Committee for Standardization, 2010) and Structural Code (Ministry of Infrastructures of the Spanish Government, 2021), and a four-time lower error than in ACI 318-19 (American Concrete Institute, 2019). A higher R^2 value at a 95% confidence (83.60%) and a lower MAE than in simple regression were obtained, while keeping the Durbin-Watson statistic above the required limit.

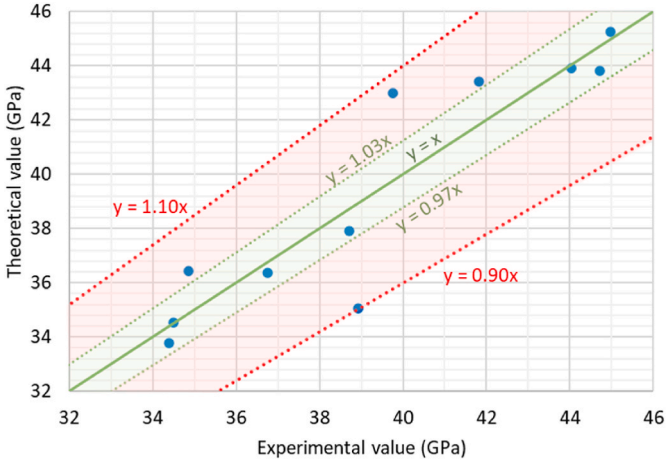

Fig. 10. Comparison between experimental values and those estimated with Equation (2).

5. Life cycle assessment

Following international standards ISO 14040/44, EN 15804, and EN 15978 (EN-Euronorm, 2020), a LCA was performed to analyze the Global Warming Potential (GWP) associated with FRC incorporating RCWTB (Manso-Morato et al., 2024). The functional unit was 1 m^3 of concrete, as usual when studying the incorporation of sustainable raw materials into concrete mixes (Acosta-Calderon et al., 2022; Frazão et al., 2022).

An open loop cradle-to-gate system boundary (A1-A3) (Xia et al., 2020) was selected, which is the most common choice among LCA practitioners (Ecoinvent Centre, 2023). This type of approach was selected as it covers all the processes at the product stage, such as raw-material study, transport and manufacturing of concrete before any construction scenario takes place, as no further information about transport to site or casting is considered in the present study (EN-Euronorm, 2020). This choice allowed the study to identify which raw materials and processes were the most environmentally demanding and aided towards tackling those precise elements.

5.1. Life cycle inventory

The Life Cycle Inventory (LCI) involved a quantification of both the inputs and the outputs during the preparation of the concrete in the laboratory. The Ecoinvent v3 (Ecoinvent Centre, 2023) database was used in SimaPro v9 software (Database and Support Teams at PRé Sustainability, 2023).

Using data from the Ecoinvent database, the cement was modeled as market for "cement, limestone 6–20%"; the mixing water was modeled as "tap water"; aggregates were modeled as market for crushed gravel or limestone; and admixtures were modeled as market for plasticizer for concrete. In addition, packaging for cement, admixture and aggregates were also introduced into the LCI, and all data were taken for Europe without Switzerland (Ecoinvent Centre, 2023). Besides, an "exclude--the-past" approach (Decorte et al., 2023) was taken for RCWTB, rendering it with no previous burdens from past choices in wind-turbine blade recycling, as those burdens are taken from past decisions that cannot be reversed (Rasmussen and Birgisdóttir, 2016) or a lack of information renders the practitioners without sufficient data to input into the LCI (Potrč Obrecht et al., 2021). The energy that was used for mixing in FRC production was modeled as market for medium voltage electricity in Spain (Ecoinvent Centre, 2023).

The transportation needed for 1 m^3 of FRC is shown in Table 10, values that were calculated through the distances between the places of acquisition and extraction of the raw materials and the laboratory: CEM II/A-L 42.5 R was purchased nearby (6.1 km); admixtures were acquired locally (6.8 km); and aggregates were extracted from the nearest quarry (26.0 km). All materials were transported in diesel truck of 16–32 metric tons payload capacity (RER, EURO4).

5.2. Life cycle impact assessment

The methodology followed for the Life Cycle Impact Assessment (LCIA) was CML-IA Baseline (CML - Department of Industrial Ecology, 2016), which studied the GWP for a potential time horizon of 100 years, expressed in equivalent kilograms of carbon dioxide ($kgCO_2e$) *per* functional unit (1 m^3 of FRC with RCWTB) at midpoint level, which only considers specific environmental burdens. This methodology is commonly used in Europe, being one of the first methodologies to be developed, and it is standard practice for FRC analysis regarding environmental performance (Manso-Morato et al., 2024). Besides, the use of a midpoint indicator such as GWP and the use of CML-IA baseline methodology allows for reduced variation of data regarding other indicators or other methodologies, providing the present study with veracity and significant results (Rybaczewska-Błażejowska and Jezierski, 2024).

Graphs showing the results appear below in Fig. 11a, while the percentile contribution of each raw material or process within each mix is depicted in Fig. 11b. The results were aligned with other research (Revilla-Cuesta et al., 2023b, 2024b), where plain concrete had an average GWP of 320 $kgCO_2e/m^3$ using ordinary Portland cement (Hafez et al., 2019), and sustainable concrete mixes incorporating the same cement type usually ranged between 208 and 404 $kgCO_2e/m^3$, with an average of 305 $kgCO_2e/m^3$ (Hafez et al., 2019). Therefore, the environmental performance of the manufactured mixes was adequate.

5.3. Discussion

The weight of cement, aggregates and RCWTB for a functional unit of 1 m^3 of FRC are expressed in Fig. 12, meanwhile Fig. 2 depicts this evolution for the water and admixtures. It may be noted that the content of some raw materials decreased (aggregates and cement) or increased (water and admixtures) when higher amounts of RCWTB were added, as those mixtures had to be empirically adjusted to obtain the desired slump. All mixes originally maintained the quantity of cement as the reference mix, although higher amounts of water and plasticizer were incorporated, that when adjusted back to an exact cubic meter, further decreased the overall decrease of the raw materials mentioned above. Those changes directly explained the variations in GWP between the different mixes.

The variation of −12.22% in the aggregate content comparing W10 to W0 resulted in a −12.35% contribution in the GWP for this raw material, meanwhile the 2.46% reduction in cement content was equated with a lower GWP contribution of 2.47%. Higher amounts of water and admixtures were needed to maintain a proper workability when using RCWTB (Ali et al., 2023), so their contributions to the GWP increased by +16.28% and +22.63%, respectively.

The overall impact of those variations was positive, as the GWP of 1 m^3 of mix W10 was 3.21% lower than that of the reference mix. The impact of cement on the GWP of the mixes varied from 243 $kgCO_2e/m^3$ in W0 to 237 $kgCO_2e/m^3$ in W10, an impact that usually represents over 75% GWP (Frazão et al., 2022; Hafez et al., 2019). Aggregates were the second most environmentally damaging raw material, whose impact ranged between 27 $kgCO_2e/m^3$ in W0 and 23 $kgCO_2e/m^3$ in W10. The average variation of GWP *per* 1% of RCWTB was 0.33%. Thus, more sustainable concrete mixes were achieved when increasing the RCWTB amount according to the LCA, apart from having defined a method of recycling wind-turbine blades and avoiding their disposal in landfills.

Table 10
LCI transportation inputs for FRC incorporating RCWTB.

Transportation (tkm)	W0	W1	W2	W3	W4	W5	W6	W7	W8	W9	W10
Cement	1.95	1.95	1.95	1.94	1.93	1.92	1.92	1.91	1.91	1.91	1.91
Admixture 1	0.007	0.007	0.007	0.007	0.007	0.007	0.008	0.008	0.008	0.009	0.009
Admixture 2	0.015	0.015	0.015	0.015	0.015	0.015	0.015	0.016	0.017	0.018	0.018
Gravel 12/22 mm	20.28	20.08	19.87	19.67	19.47	19.27	19.06	18.86	18.66	18.46	18.25
Gravel 4/12 mm	14.43	14.29	14.14	14.00	13.85	13.71	13.56	13.42	13.28	13.13	12.99
Sand 0/4 mm	10.01	9.91	9.81	9.71	9.61	9.51	9.41	9.31	9.21	9.11	9.01
Sand 0/2 mm	7.28	7.21	7.13	7.06	6.99	6.92	6.84	6.77	6.70	6.63	6.55
RCWTB	0.00	0.08	0.16	0.24	0.32	0.40	0.49	0.57	0.65	0.73	0.81

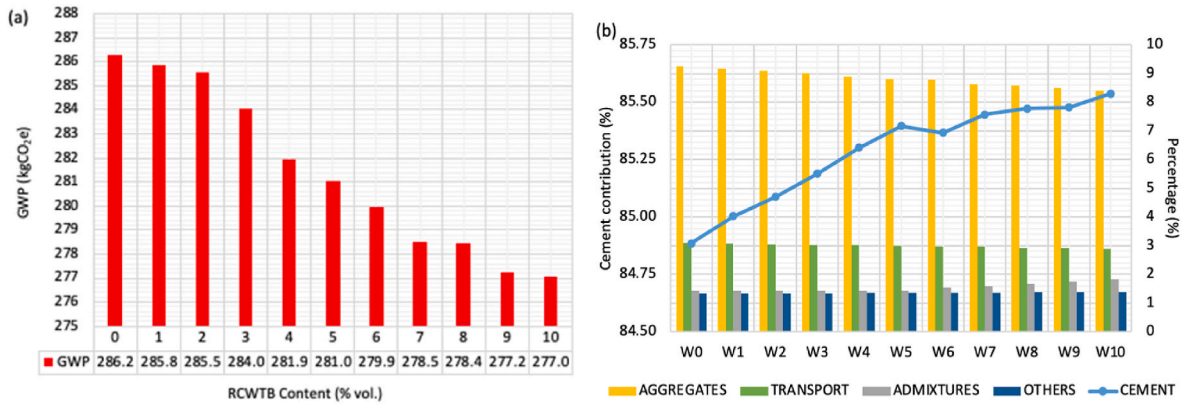

Fig. 11. GWP: (a) values; (b) Percentile contribution of each raw material or process.

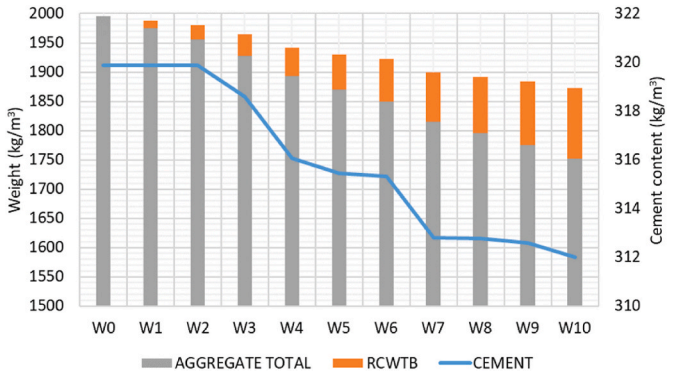

Fig. 12. Weight of aggregates, RCWTB, and cement for 1 m^3 of concrete.

When comparing to other LCA research incorporating conventional fibers (steel, glass or propylene) into concrete mixes with a cradle-to-gate approach (A1-A3), it is noticeable that mixes containing RCWTB had a lower GWP at all cases, with enhanced mechanical characteristics (Ali et al., 2023). When compared to 1% vol. steel fiber-reinforced concrete, GWP was reduced up to 51.48%; comparing to 1% vol. glass fiber-reinforced concrete, the reduction of GWP was up to 33.25%; and lastly, when comparing with 1% vol. propylene fibers, the reduction was up to 26.70% (Ali et al., 2023). In addition, when compared to recycled fibers, such as recycled tire-steel fibers in a similar dosage (75.8 kg/m^3 of recycled fibers), GWP of concrete was also reduced up to 30.27% by applying the same LCA approach, while achieving similar mechanical properties (Frazão et al., 2022). Finally, when comparing the results with natural fiber-reinforced concrete using 0.6 kg/m^3 sisal fibers (Acosta-Calderon et al., 2022), GWP was reduced up to 11.71%, while enhancing mechanical properties. Therefore, concrete mixes containing RCWTB not only had proper fresh-state and mechanical behavior but also did perform better in terms of LCA than other mixes incorporating different types of fibers.

However, it is important to highlight the limitations of the LCA in this study. Data collection and transportation burdens were used for the exposed dosage of FRC and the exact manufacturing site, thus being necessary to adapt distances and specific data taken from the used database to best represent the specific case under study. The approach and system boundaries taken are also important choices towards final LCA results, being the cradle-to-gate the most representative one in this case, but further research needs to be done regarding a cradle-to-grave approach, in which all impacts during the full life cycle of concrete incorporating RCWTB are considered. Lastly, it is important to mention that no data regarding environmental burdens of wind-turbine blade mechanical recycling were found in the literature, showing the novelty of this study and a clear path towards the next steps of this research line.

6. Conclusions

A full mechanical and environmental characterization of concrete containing high amounts of RCWTB (up to 10%) at an age of 28 days has been conducted in the present research. Proper adjustment of the contents of water and admixtures has ensured an adequate workability of the mixes when adding this waste in the form of non-selectively crushed wind-turbine blades, meanwhile a three-step mixing process guaranteed its homogeneous distribution in the concrete mass. The following conclusions can be drawn from this research:

- The lower density of RCWTB and the air entrainment ability of the GFRP-composite fibers that it contained slightly decreased the fresh density and increased the occluded air content. The hardened density followed a similar decreasing trend, although adequate density levels (around 2.3 kg/dm^3) were reached.
- Compressive strength showed a slight decreasing trend as higher amounts of RCWTB were added. However, the addition of low RCWTB amounts (2% in this research) improved overall strength, while the compressive strength remained approximately constant for RCWTB contents between 4% and 10%. High amounts of RCWTB could therefore be added to concrete without excessively hindering its compressive strength.
- Tensile splitting strength was enhanced by the presence of GFRP-composite fibers in the RCWTB by up to 6.44%, while flexural strength was maintained. The fibers bridged the cementitious matrix, so that the concrete had a more ductile behavior.
- RCWTB additions resulted in higher longitudinal strains and less bulging under axial loads, so lower moduli of elasticity and Poisson's coefficients were recorded. The presence of deformable particles in the RCWTB negatively affected the stiffness in the longitudinal direction, while the fibers reduced bulging in the transverse direction.
- A regression model using compressive strength as an independent variable and the hardened density as a correction factor predicted the modulus of elasticity with an average deviation of 3.11%. The highest Pearson's correlation coefficients were registered between those three properties.
- Life cycle analysis yielded a 3.21% reduction in GWP when adding 10% RCWTB to concrete. The amounts of cement and aggregates were reduced when adding this waste, although higher amounts of water and admixtures had to be incorporated.

In conclusion, RCWTB has successfully been added to concrete in amounts up to 10%, although its content should be defined according to the mechanical and environmental properties to be improved. Low contents conserved compressive strength, while high contents increased

tensile splitting strength. Flexural strength never decreased when adding RCWTB, and GWP was always reduced. These results have clearly demonstrated that increased concrete production over future years could greatly benefit from the addition of RCWTB, while avoiding the disposal of wind-turbine blades at landfill sites. Nevertheless, ongoing research is needed with regard to long-term strength development, durability assessment, and stress-strain evaluation of the concrete produced with this waste.

CRediT authorship contribution statement

Javier Manso-Morato: Writing – original draft, Validation, Methodology, Investigation, Formal analysis, Conceptualization. **Nerea Hurtado-Alonso:** Visualization, Validation, Software, Methodology, Investigation, Formal analysis. **Víctor Revilla-Cuesta:** Writing – review & editing, Visualization, Software, Methodology, Investigation, Formal analysis. **Vanesa Ortega-López:** Writing – review & editing, Supervision, Resources, Project administration, Funding acquisition, Conceptualization.

Declaration of competing interest

The authors declare that they have no known competing financial interests or personal relationships that could have appeared to influence the work reported in this paper.

Acknowledgments

This research work was supported by the Spanish Ministry of Universities, MICINN, AEI, EU, ERDF and NextGenerationEU/PRTR [grant numbers PID2020-113837RB-I00; 10.13039/501100011033; TED2021-129715 B–I00; PID2023-146642OB-I00; FPU21/04364]; the Junta de Castilla y León (Regional Government) and ERDF [grant number UIC-231; BU033P23; BU066-22]; and, finally, the University of Burgos [grant number SUCONS, Y135. GI].

Data availability

Data will be made available on request.

References

Abdolpour, H., Muthu, M., Niewiadomski, P., Sadowski, Ł., Hojdys, Ł., Krajewski, P., Kwiecień, A., 2023. Performance and life cycle of ultra-high performance concrete mixes containing oil refinery waste catalyst and steel fibre recovered from scrap tyre. J. Build. Eng. 79, 107890. https://doi.org/10.1016/j.jobe.2023.107890.

Acosta-Calderon, S., Gordillo-Silva, P., García-Troncoso, N., Bompa, D.V., Flores-Rada, J., 2022. Comparative evaluation of sisal and polypropylene fiber reinforced concrete properties. Fibers 10, 31. https://doi.org/10.3390/fib10040031.

Ali, B., Ahmed, H., Hafez, H., Brahmia, A., Ouni, M.H.E., Raza, A., 2023. Life cycle impact assessment (Cradle-to-Gate) of fiber-reinforced concrete application for pavement use: a case study of islamabad city. Int. J. Pavement Eng. 16, 247–263. https://doi.org/10.1007/s42947-021-00129-8.

Alsaif, A., Alharbi, Y.R., 2022. Strength, durability and shrinkage behaviours of steel fiber reinforced rubberized concrete. Construct. Build. Mater. 345, 128295. https://doi.org/10.1016/j.conbuildmat.2022.128295.

American Concrete Institute, 2019. ACI 318-19: Building Code Requirements for Structural Concrete: Commentary on Building Code Requirements for Structural Concrete (ACI 318R-19). ACI, Michigan, USA.

ANEFHOP, 2022. Guide for the Carbon Footprint Reduction in the Prepared Concrete Industry (GUÍA PARA LA REDUCCIÓN DE LA HUELLA DE CARBONO DE LA INDUSTRIA DEL HORMIGÓN PREPARADO).

Barbudo, A., de Brito, J., Evangelista, L., Bravo, M., Agrela, F., 2013. Influence of water-reducing admixtures on the mechanical performance of recycled concrete. J. Clean. Prod. 59, 93–98. https://doi.org/10.1016/j.jclepro.2013.06.022.

Baturkin, D., Hisseine, O.A., Masmoudi, R., Tagnit-Hamou, A., Massicotte, L., 2021. Valorization of recycled FRP materials from wind turbine blades in concrete. Resour. Conserv. Recycl. 174, 105807. https://doi.org/10.1016/j.resconrec.2021.105807.

Beauson, J., Brøndsted, P., 2016. Wind turbine blades: an end of life perspective. In: MARE-WINT. Springer International Publishing, pp. 421–432. https://doi.org/10.1007/978-3-319-39095-6_23.

Behera, M., Bhattacharyya, S.K., Minocha, A.K., Deoliya, R., Maiti, S., 2014. Recycled aggregate from C&D waste & its use in concrete – a breakthrough towards sustainability in construction sector: a review. Construct. Build. Mater. 68, 501–516. https://doi.org/10.1016/j.conbuildmat.2014.07.003.

CML - Department of Industrial Ecology, 2016. CML-IA characterisation factors [WWW Document]. URL. https://www.universiteitleiden.nl/en/research/research-output/science/cml-ia-characterisation-factors. accessed 10.30.23.

Correia, J.R., Almeida, N.M., Figueira, J.R., 2011. Recycling of FRP composites: reusing fine GFRP waste in concrete mixtures. J. Clean. Prod. 19, 1745–1753. https://doi.org/10.1016/j.jclepro.2011.05.018.

Database and Support Teams at PRé Sustainability, 2023. SimaPro 9.5. What's New?.

Decorte, Y., Van Den Bossche, N., Steeman, M., 2023. Guidelines for defining the reference study period and system boundaries in comparative LCA of building renovation and reconstruction. Int. J. Life Cycle Assess. 28, 111–130. https://doi.org/10.1007/s11367-022-02114-0.

di Prisco, M., Plizzari, G., Vandewalle, L., 2009. Fibre reinforced concrete: new design perspectives. Mater. Struct. 42, 1261–1281. https://doi.org/10.1617/s11527-009-9529-4.

Ecoinvent Centre, 2023. Ecoinvent database [WWW Document]. URL. https://ecoinvent.org/the-ecoinvent-database/. accessed 10.31.23.

EN-Euronorm, 2020. European comittee for standardization. Rue de Stassart 36. Belgium-1050 Burssels.

Esmizadeh, E., Khalili, S., Vahidifar, A., Naderi, G., Dubois, C., 2019. Waste polymethyl methacrylate (PMMA): recycling and high-yield monomer recovery. In: Martínez, L. M.T., Kharissova, O.V., Kharisov, B.I. (Eds.), Handbook of Ecomaterials. Springer International Publishing, Cham, pp. 2977–3009. https://doi.org/10.1007/978-3-319-68255-6_164.

European Committee for Standardization, 2010. Eurocode 2, Design of Concrete Structures. Part 1-1: General Rules and Rules for Buildings (EN 1992-1-1).

Faleschini, F., Trento, D., Zanini, M.A., Pellegrino, C., Ortega-López, V., Santamaria, A., 2023. Mechanical strength and environmental sustainability of EAF concrete. In: Life-Cycle of Structures and Infrastructure Systems. CRC Press, London, pp. 2455–2462. https://doi.org/10.1201/9781003323020-299.

Ferronato, N., Torretta, V., 2019. Waste mismanagement in developing countries: a review of global issues. Int. J. Environ. Res. Publ. Health 16, 1060. https://doi.org/10.3390/ijerph16061060.

Frazão, C., Barros, J., Bogas, J.A., García-Cortés, V., Valente, T., 2022. Technical and environmental potentialities of recycled steel fiber reinforced concrete for structural applications. J. Build. Eng. 45, 103579. https://doi.org/10.1016/j.jobe.2021.103579.

Gu, L., Ozbakkaloglu, T., 2016. Use of recycled plastics in concrete: a critical review. Waste Manag. 51, 19–42. https://doi.org/10.1016/j.wasman.2016.03.005.

Habert, G., Denarié, E., Šajna, A., Rossi, P., 2013. Lowering the global warming impact of bridge rehabilitations by using ultra high performance fibre reinforced concretes. Cem. Concr. Compos. 38, 1–11. https://doi.org/10.1016/j.cemconcomp.2012.11.008.

Hafez, H., Kurda, R., Cheung, W.M., Nagaratnam, B., 2019. A systematic review of the discrepancies in life cycle assessments of green concrete. Appl. Sci. 9, 4803. https://doi.org/10.3390/app9224803.

Hay, R., Ostertag, C.P., 2018. Life cycle assessment (LCA) of double-skin façade (DSF) system with fiber-reinforced concrete for sustainable and energy-efficient buildings in the tropics. Build. Environ. 142, 327–341. https://doi.org/10.1016/j.buildenv.2018.06.024.

Hofmeister, M., 2012. Recycling Turbine Blade Composites: Concrete Aggregate and Reinforcement. Tech.

Islam, MdJ., Shahjalal, Md, Haque, N.M.A., 2022. Mechanical and durability properties of concrete with recycled polypropylene waste plastic as a partial replacement of coarse aggregate. J. Build. Eng. 54, 104597. https://doi.org/10.1016/j.jobe.2022.104597.

Joustra, J., Flipsen, B., Balkenende, R., 2021. Structural reuse of wind turbine blades through segmentation. Composites Part C 5, 100137. https://doi.org/10.1016/J.JCOMC.2021.100137.

Juenger, M.C.G., Siddique, R., 2015. Recent advances in understanding the role of supplementary cementitious materials in concrete. Cement Concr. Res. 78, 71–80. https://doi.org/10.1016/j.cemconres.2015.03.018.

Khelifa, M.-R., Ziane, S., Mezhoud, S., Ledesert, C., Hebert, R., Ledesert, B., 2021. Compared environmental impact analysis of alfa and polypropylene fibre-reinforced concrete. IJST-T CIV. ENG. 45, 1511–1522. https://doi.org/10.1007/s40996-020-00555-x.

Khodabakhshian, A., de Brito, J., Ghalehnovi, M., Asadi Shamsabadi, E., 2018. Mechanical, environmental and economic performance of structural concrete containing silica fume and marble industry waste powder. Construct. Build. Mater. 169, 237–251. https://doi.org/10.1016/j.conbuildmat.2018.02.192.

Kirthika, S.K., Singh, S.K., Chourasia, A., 2020. Alternative fine aggregates in production of sustainable concrete- A review. J. Clean. Prod. 268, 122089. https://doi.org/10.1016/j.jclepro.2020.122089.

Kurda, R., Silvestre, J.D., de Brito, J., 2018. Life cycle assessment of concrete made with high volume of recycled concrete aggregates and fly ash. Resour. Conserv. Recycl. 139, 407–417. https://doi.org/10.1016/j.resconrec.2018.07.004.

Leon, M.J., 2023. Recycling of wind turbine blades: recent developments. Curr. Opin. Green Sustain. Chem. 39, 100746. https://doi.org/10.1016/j.cogsc.2022.100746.

Liu, F., Ding, W., Qiao, Y., 2020. Experimental investigation on the tensile behavior of hybrid steel-PVA fiber reinforced concrete containing fly ash and slag powder. Construct. Build. Mater. 241, 118000. https://doi.org/10.1016/J.CONBUILDMAT.2020.118000.

Mahdi, S., Xie, T., Venkatesan, S., Gravina, R.J., 2023. Mechanical characterisation and small-scale life-cycle assessment of polypropylene macro-fibre blended recycled

cardboard concrete. Construct. Build. Mater. 409, 133902. https://doi.org/10.1016/j.conbuildmat.2023.133902.
Manso-Morato, J., Hurtado-Alonso, N., Revilla-Cuesta, V., Skaf, M., Ortega-López, V., 2024. Fiber-Reinforced concrete and its life cycle assessment: a systematic review. J. Build. Eng. 94, 110062. https://doi.org/10.1016/j.jobe.2024.110062.
Martínez-Lage, I., Vázquez-Burgo, P., Velay-Lizancos, M., 2020. Sustainability evaluation of concretes with mixed recycled aggregate based on holistic approach: technical, economic and environmental analysis. Waste Manag. 104, 9–19. https://doi.org/10.1016/j.wasman.2019.12.044.
Merli, R., Preziosi, M., Acampora, A., Lucchetti, M.C., Petrucci, E., 2020. Recycled fibers in reinforced concrete: a systematic literature review. J. Clean. Prod. 248, 119207. https://doi.org/10.1016/j.jclepro.2019.119207.
Migliore, Marco, Talamo, Cinzia, Paganin, Giancarlo, 2019. Strategies for circular economy and cross-sectoral exchanges for sustainable building - products preventing and recycling waste. In: Springer Tracts in Civil Engineering, first ed. Springer International Publishing, Cham. https://doi.org/10.1007/978-3-030-30318-1. 2019.
Miller, S.A., Monteiro, P.J.M., Ostertag, C.P., Horvath, A., 2016. Concrete mixture proportioning for desired strength and reduced global warming potential. Construct. Build. Mater. 128, 410–421. https://doi.org/10.1016/j.conbuildmat.2016.10.081.
Ministry of Infrastructures of the Spanish Government, 2021. Spanish Structural Code (Código Estructural de España).
Mousavi, S.M., Ranjbar, M.M., Madandoust, R., 2019. Combined effects of steel fibers and water to cementitious materials ratio on the fracture behavior and brittleness of high strength concrete. Eng. Fract. Mech. 216, 106517. https://doi.org/10.1016/j.engfracmech.2019.106517.
Muthukumarana, T.V., Arachchi, M.A.V.H.M., Somarathna, H.M.C.C., Raman, S.N., 2023. A review on the variation of mechanical properties of carbon fibre-reinforced concrete. Construct. Build. Mater. 366, 130173. https://doi.org/10.1016/j.conbuildmat.2022.130173.
Nagle, A.J., Delaney, E.L., Bank, L.C., Leahy, P.G., 2020. A Comparative Life Cycle Assessment between landfilling and Co-Processing of waste from decommissioned Irish wind turbine blades. J. Clean. Prod. 277, 123321. https://doi.org/10.1016/j.jclepro.2020.123321.
Nedeljković, M., Visser, J., Šavija, B., Valcke, S., Schlangen, E., 2021. Use of fine recycled concrete aggregates in concrete: a critical review. J. Build. Eng. 38, 102196. https://doi.org/10.1016/j.jobe.2021.102196.
Neocleous, K., Angelakopoulos, H., Pilakoutas, K., Guadagnin, M., 2011. Fibre-reinforced roller compacted concrete transport pavements. Proc. Inst. Civ. Eng.: Transport 164, 97–109. https://doi.org/10.1680/tran.9.00043.
Ortega-López, V., Revilla-Cuesta, V., Santamaría, A., Orbe, A., Skaf, M., 2022. Microstructure and dimensional stability of slag-based high-workability concrete with steelmaking slag aggregate and fibers. J. Mater. Civ. Eng. 34, 04022224. https://doi.org/10.1061/(ASCE)MT.1943-5533.0004372.
Peceño, B., Leiva, C., Alonso-Fariñas, B., Gallego-Schmid, A., 2020. Is recycling always the best option? Environmental assessment of recycling of seashell as aggregates in noise barriers. Processes 8, 776. https://doi.org/10.3390/pr8070776.
Petit, A., Cordoba, G., Paulo, C.I., Irassar, E.F., 2018. Novel air classification process to sustainable production of manufactured sands for aggregate industry. J. Clean. Prod. 198, 112–120. https://doi.org/10.1016/J.JCLEPRO.2018.07.010.
PlasticsEurope, E., 2019. Plastics—the facts 2019. An analysis of European plastics production, demand and waste data. PlasticEurope. https://www.plasticseurope.org/en/resources/publications/1804-plastics-facts-2019.
Potrč Obrecht, T., Jordan, S., Legat, A., Passer, A., 2021. The role of electricity mix and production efficiency improvements on greenhouse gas (GHG) emissions of building components and future refurbishment measures. Int. J. Life Cycle Assess. 26, 839–851. https://doi.org/10.1007/s11367-021-01920-2.
Pradhan, S., Tiwari, B.R., Kumar, S., Barai, S.V., 2019. Comparative LCA of recycled and natural aggregate concrete using Particle Packing Method and conventional method of design mix. J. Clean. Prod. 228, 679–691. https://doi.org/10.1016/J.JCLEPRO.2019.04.328.
Rasmussen, F.N., Birgisdóttir, H., 2016. Life cycle environmental impacts from refurbishment projects-A case study. In: Central Europe towards Sustainable Building 2016: CESB 2016: Innovations for Sustainable Future. GRADA PUBLISHING, pp. 277–284.
Revilla-Cuesta, V., Fiol, F., Perumal, P., Ortega-López, V., Manso, J.M., 2022a. Using recycled aggregate concrete at a precast-concrete plant: a multi-criteria company-oriented feasibility study. J. Clean. Prod. 373, 133873. https://doi.org/10.1016/j.jclepro.2022.133873.
Revilla-Cuesta, V., Shi, J., Skaf, M., Ortega-López, V., Manso, Juan Manuel, 2022b. Non-destructive density-corrected estimation of the elastic modulus of slag-cement self-compacting concrete containing recycled aggregate. Dev. Built. Environ. 12, 100097. https://doi.org/10.1016/j.dibe.2022.100097.
Revilla-Cuesta, V., Serrano-López, R., Espinosa, Ana Belén, Ortega-López, V., Skaf, M., 2023a. Analyzing the relationship between compressive strength and modulus of elasticity in concrete with ladle furnace slag. Buildings 13, 3100. https://doi.org/10.3390/buildings13123100.
Revilla-Cuesta, V., Skaf, M., Ortega-López, V., Manso, J.M., 2023b. Raw-crushed wind-turbine blade: waste characterization and suitability for use in concrete production. Resour. Conserv. Recycl. 198, 107160. https://doi.org/10.1016/j.resconrec.2023.107160.
Revilla-Cuesta, V., Faleschini, F., Pellegrino, C., Skaf, M., Ortega-López, V., 2024a. Water transport and porosity trends of concrete containing integral additions of raw-crushed wind-turbine blade. Dev. Built Environ. 17, 100374. https://doi.org/10.1016/j.dibe.2024.100374.
Revilla-Cuesta, V., Manso-Morato, J., Hurtado-Alonso, N., Skaf, M., Ortega-López, V., 2024b. Mechanical and environmental advantages of the revaluation of raw-crushed wind-turbine blades as a concrete component. J. Build. Eng. 82, 108383. https://doi.org/10.1016/j.jobe.2023.108383.
Rybaczewska-Błażejowska, M., Jezierski, D., 2024. Comparison of ReCiPe 2016, ILCD 2011, CML-IA baseline and IMPACT 2002+ LCIA methods: a case study based on the electricity consumption mix in Europe. Int. J. Life Cycle Assess. 29, 1799–1817. https://doi.org/10.1007/s11367-024-02326-6.
Sadler, R.L., Sharpe, M., Panduranga, R., Shivakumar, K., 2009. Water immersion effect on swelling and compression properties of Eco-Core, PVC foam and balsa wood. Compos. Struct. 90, 330–336. https://doi.org/10.1016/j.compstruct.2009.03.016.
Sahmaran, M., Yurtseven, A., Ozgur Yaman, I., 2005. Workability of hybrid fiber reinforced self-compacting concrete. Build. Environ. 40, 1672–1677. https://doi.org/10.1016/j.buildenv.2004.12.014.
Schober, P., Boer, C., Schwarte, L.A., 2018. Correlation coefficients: appropriate use and interpretation. Anesth. Analg. 126, 1763–1768. https://doi.org/10.1213/ANE.0000000000002864.
Shi, F., Pham, T.M., Hao, H., Hao, Y., 2020. Post-cracking behaviour of basalt and macro polypropylene hybrid fibre reinforced concrete with different compressive strengths. Construct. Build. Mater. 262, 120108. https://doi.org/10.1016/j.conbuildmat.2020.120108.
Shilov, A.V., Beskopylny, A.N., Meskhi, B., Mailyan, D., Shilov, D., Polushkin, O.O., 2021. Ultimate compressive strains and reserves of bearing capacity of short RC columns with basalt fiber. Appl. Sci. 11, 7634. https://doi.org/10.3390/app11167634.
Signorini, C., Marinelli, S., Volpini, V., Nobili, A., Radi, E., Rimini, B., 2022. Performance of concrete reinforced with synthetic fibres obtained from recycling end-of-life sport pitches. J. Build. Eng. 53, 104522. https://doi.org/10.1016/j.jobe.2022.104522.
Silva, R.V., de Brito, J., Dhir, R.K., 2016. Establishing a relationship between modulus of elasticity and compressive strength of recycled aggregate concrete. J. Clean. Prod. 112, 2171–2186. https://doi.org/10.1016/j.jclepro.2015.10.064.
Soltanzadeh, F., Behbahani, A.E., Hosseinmostofi, K., Teixeira, C.A., 2022. Assessment of the sustainability of fibre-reinforced concrete by considering both environmental and mechanical properties. Sustainability 14, 6347. https://doi.org/10.3390/su14106347.
Vieira, D.R., Calmon, J.L., Coelho, F.Z., 2016. Life cycle assessment (LCA) applied to the manufacturing of common and ecological concrete: a review. Construct. Build. Mater. 124, 656–666. https://doi.org/10.1016/J.CONBUILDMAT.2016.07.125.
World Wind Energy Association, 2022. WWEA, 2022. Statistics for the Global Wind-Energy Sector [WWW Document].
Xia, B., Ding, T., Xiao, J., 2020. Life cycle assessment of concrete structures with reuse and recycling strategies: a novel framework and case study. Waste Manag. 105, 268–278. https://doi.org/10.1016/j.wasman.2020.02.015.
Xing, W., Tam, V.W., Le, K.N., Hao, J.L., Wang, J., 2023. Life cycle assessment of sustainable concrete with recycled aggregate and supplementary cementitious materials. Resour. Conserv. Recycl. 193, 106947. https://doi.org/10.1016/J.RESCONREC.2023.106947.
Yazdanbakhsh, A., Bank, L.C., Chen, C., Tian, Y., 2017. FRP-Needles as discrete reinforcement in concrete. J. Mater. Civ. Eng. 29, 04017175. https://doi.org/10.1061/(ASCE)MT.1943-5533.0002033.
Yina, S., Tuladhar, R., Sheehan, M., Combe, M., Collister, T., 2016. A life cycle assessment of recycled polypropylene fibre in concrete footpaths. J. Clean. Prod. 112, 2231–2242. https://doi.org/10.1016/j.jclepro.2015.09.073.
Yu, Y., Zheng, Y., Xu, J., Wang, X., 2021. Modeling and predicting the mechanical behavior of concrete under uniaxial loading. Construct. Build. Mater. 273, 121694. https://doi.org/10.1016/j.conbuildmat.2020.121694.
Yuan, H., Zhu, L., Zhang, M., Wang, X., 2023. Mechanical behavior and environmental assessment of steel-bars truss slab using steel fiber-reinforced recycled concrete. J. Build. Eng. 69, 106252. https://doi.org/10.1016/j.jobe.2023.106252.
Zhong, H., Zhang, M., 2020. Experimental study on engineering properties of concrete reinforced with hybrid recycled tyre steel and polypropylene fibres. J. Clean. Prod. 259, 120914. https://doi.org/10.1016/J.JCLEPRO.2020.120914.